Parabolic Equations for Atmospheric Waves

J.F. Lingevitch,[1] M.D. Collins,[1] D.K. Dacol,[1]
D.P. Drob,[1] J.C.W. Rogers,[2] and
W.L. Siegmann[3]
[1]*Acoustics Division*
[2]*Polytechnic University*
[3]*Rensselaer Polytechnic Institute*

Introduction: The Earth's atmosphere is a complex dynamical system supporting a wide variety of wave phenomena. The study and understanding of such waves is aided by computer simulations in which controlled experiments under ideal conditions can be conducted to isolate physical effects and test hypotheses governing the real atmosphere. Even so, the numerical solution of the equations governing atmospheric waves is computationally expensive and requires simplification of the full hydrodynamic wave equations. A common approach in the study of atmospheric waves is to solve a linearized model about a representative atmospheric state using the methods of ray theory. Ray theory is an efficient technique for high frequencies but becomes less accurate when the length scales of atmospheric features are comparable to the acoustic wavelength. In this article we demonstrate another approach, the method of parabolic equations, for solving atmospheric wave equations. The parabolic equation method is an efficient and accurate solution technique and is not constrained by the asymptotic frequency restrictions of ray theory. We show that the parabolic equation method can be applied to atmospheric acousto-gravity (AG) waves and to acoustic waves in horizontal shear flow. This work improves previous implementations of parabolic equations, which were restricted to narrow propagation angles and low Mach number.

Parabolic Equation Method: The parabolic equation method was pioneered in the 1940s for the study of radio waves in the atmosphere. Since that time, the method has been extended to a wider class of wave phenomena, including ocean acoustics, geoacoustics, electromagnetics, and scattering problems. The method is based on factoring the wave equation into incoming and outgoing components. When one component of the wave dominates, as is often the case for a wave generated by a localized source, the factored equation can be solved orders of magnitude more efficiently than the full elliptic wave equation. This is important when the scale of the computational domain is many acoustic wavelengths. A parabolic equation is efficiently solved by advancing the field in range with a marching algorithm.

Applications to Atmospheric Problems: We apply the parabolic equation method to several problems involving atmospheric waves using a realistic model of the Earth's atmosphere. First, we consider the case of infrasonic AG waves in a stratified atmosphere with no horizontal background flow. A two-dimensional geometry is considered; the vertical coordinate is altitude above a rigid Earth, and the horizontal coordinate is range from an infrasonic acoustic source. The absorption in the upper atmosphere is inversely proportional to molecular density, so energy propagating at high angles is rapidly attenuated. Figure 1(a) shows the density, sound speed, and buoyancy frequency profiles. A parcel of fluid displaced vertically from its equilibrium position will oscillate at the local buoyancy frequency. Figure 1(b) contains two intensity plots for the 3 MHz source located 10 km above the rigid Earth. The bottom left figure shows an AG wave, and the bottom right figure shows a pure gravity wave in which the compressibility effects are neglected. At infrasonic frequencies close to the buoyancy frequency of the atmosphere, the combined effects of gravity and medium compressibility lead to hybrid AG waves that are significantly different from pure gravity or acoustic waves. The main difference in this case is due to a surface wave that decays exponentially with altitude (a Lamb wave) in the AG wavenumber spectrum that is not present in the gravity wavenumber spectrum.

Parabolic equations are also applicable to problems involving range-varying atmospheric profiles or topography. Range-dependent propagation is handled by enforcing single-scattering continuity conditions on the pressure and displacement at ranges where the profiles are updated. This method accounts for first-order scattering caused by the range dependence. Multiple scattering effects are negligible if the range dependence is sufficiently weak. Figure 2 shows an example demonstrating mode coupling resulting from range-dependent propagation over a simulated mountain range. The topographical variations occur at ranges between 100 and 340 km, with a maximum altitude of 3 km. A 3 MHz Lamb wave is incident on a simulated mountain range. Coupling induced by the mountains excites a mode that interferes with the original Lamb wave in the upper atmosphere.

Horizontal shear flow in the atmosphere can significantly affect infrasonic acoustic propagation. The top panel of Fig. 3 shows density, sound speed, and wind speed profiles obtained from measurements and

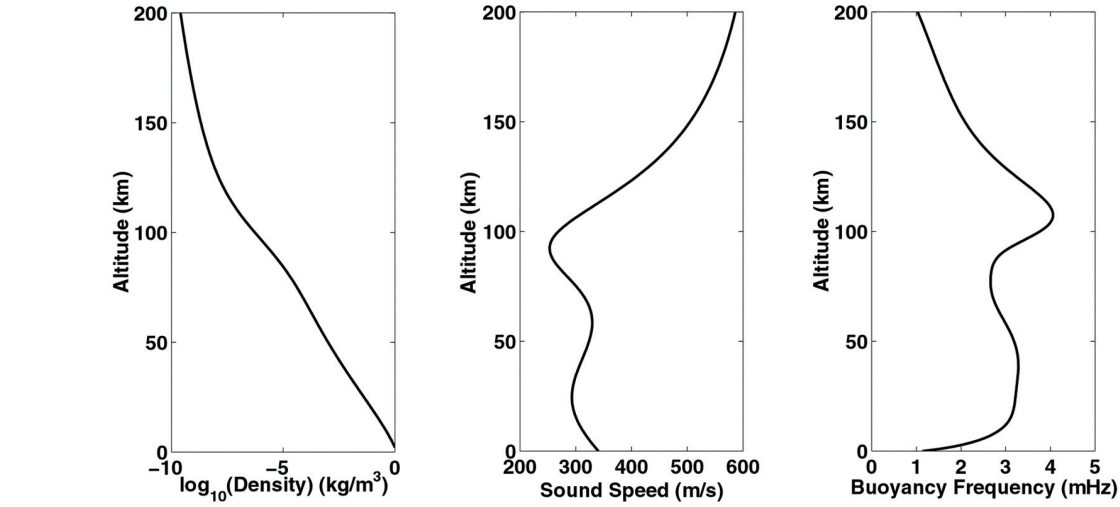

(a)

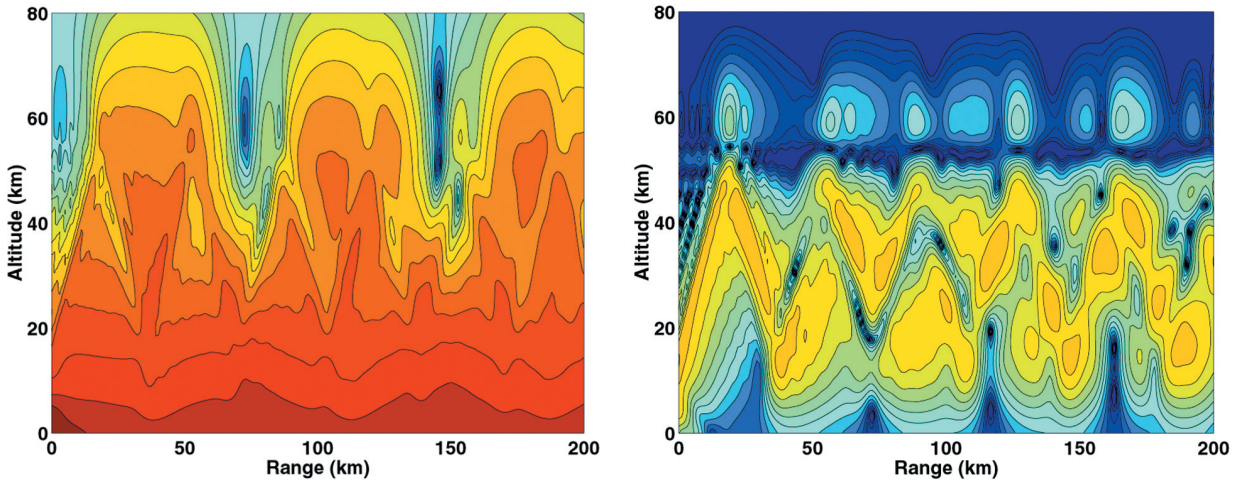

(b)

FIGURE 1
(a) Model atmospheric profiles for density, sound speed, and buoyancy frequency obtained by smoothing tabulated standard atmospheric profiles. (b) Intensity plots of 3-MHz (left) AG and (right) pure gravity waves. The AG wave contains a large amount of energy near the ground due to a contribution of the Lamb wave; dynamic range of the plots is 50 dB.

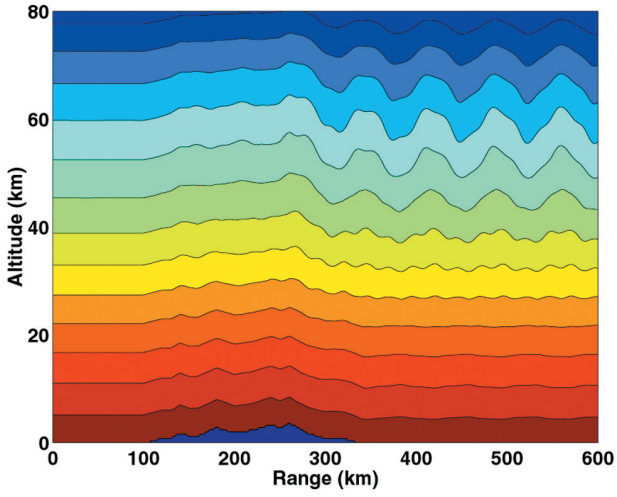

FIGURE 2
Intensity plot for a 3 MHz Lamb wave propagating over variable topography. The range-dependence induces mode coupling as can be seen from the modal interference pattern; dynamic range of the plot is 25 dB.

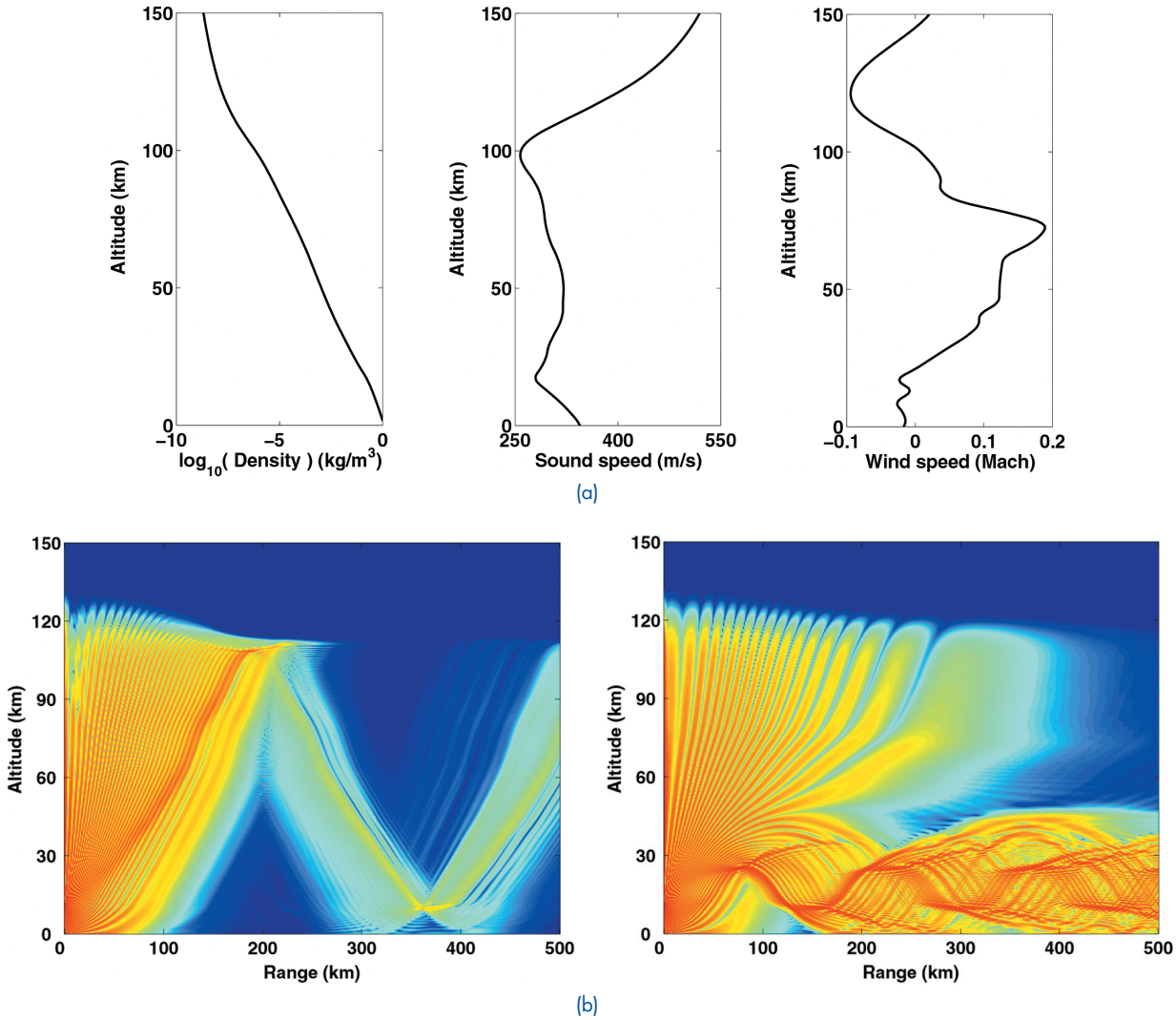

FIGURE 3
(a) Representative density, sound speed, and wind speed profiles obtained from measurement and models (top row). Intensity plots for an outward-propagating wave are due to a 0.5 Hz source. (b) The left shows the energy propagating in the upwind direction (to the left) and the right is the energy propagating in the downward direction (to the right). The dynamic range of the plot is 70 dB.

models developed by the Upper Atmospheric Physics group at NRL (Code 7640). The noncommutativity of the shear and acoustic operators in the advected wave equation complicates the derivation of the parabolic equation in this case. An approximate factorization that is accurate to leading order in the commutator is derived from the spectral solution. The bottom panel of Fig. 3 shows the upwind/downwind comparison of the acoustic field and illustrates the dramatic influence of a wind profile on an infrasonic acoustic wave.

Summary: We have derived parabolic equations for problems involving acoustic and gravity waves in the atmosphere. The effects of horizontal shear have also been incorporated into a wide-angle high-Mach-number parabolic equation. Parabolic equation methods combine accuracy and efficiency for solving range-dependent wave propagation problems and are applicable at infrasonic frequencies where ray methods are inaccurate.

[Sponsored by ONR]

References

[1] J.F. Lingevitch, M.D. Collins, and W.L. Siegmann, "Parabolic Equations for Gravity and Acousto-gravity Waves," *J. Acoust. Soc. Am.* **105**, 3049-3056 (1999).

[2] J.F. Lingevitch, M.D. Collins, D.K. Dacol, D.P. Drob, J.C.W. Rogers, and W.L. Siegmann, "A Wide Angle and High Mach Number Parabolic Equation," *J. Acoust. Soc. Am.* (in press).

Perturbation of the Littoral Sound Speed Field by Small-Scale Shelf/Slope Fluid Processes

M.H. Orr and P.C. Mignerey
Acoustics Division

Introduction: We have been studying the small-scale fluid processes that periodically perturb the ocean's sound speed field in the vicinity of the continental shelf break. A high-frequency acoustic backscattering system is used to generate flow visualization images of the processes. The images are used to estimate their impact on the sound speed field variability. A correlation between the occurrence of the small-scale fluid processes and the tidal flow has been observed. Due to the periodicity of the tide, it is felt that we may eventually develop an ability to estimate the variability of both the sound speed field and the acoustic signals that propagate through it. As a result, we may be able to estimate the performance of Navy acoustic antisubmarine warfare (ASW) systems operating in littoral areas.

Fluid Processes: The shelf/slope water column is often composed of layers of water of differing density or sound speed. The layers have range-dependent thickness variability. Navy sonar operators usually treat the layers as time invariant, i.e., that there is no time dependent change in thickness or vertical displacement of the layers. The layers can, however, be temporally perturbed (vertically displaced) as the result of tidal flow over sloping ocean bottoms.

A sharp discontinuity in water depth occurs at the shelf/slope break. Tidal flow over the break causes the layers of water to be displaced in the vertical. The displacement generates waves that displace the interfaces between the water layers and propagate away from the shelf break. These waves are called internal waves because they do not noticeably displace the air/sea interface surface as do ocean surface waves. The internal waves are generated on every tide and propagate away from the shelf/slope break with a known speed. Consequently, their distance from the shelf break can be calculated and their influence on the shelf and slope sound speed profile can be estimated.

If there are several water layers, the layers can be vertically displaced by internal waves in a variety of ways. If all the layers are displaced together vertically upward or downward, the displacement is called a mode 1 internal wave. If the top boundary of a layer is displaced upward and the bottom bondary of a layer is displaced downward, the displacement is called a mode 2 internal wave.

Acoustic Flow Visualization: Two-hundred kHz acoustic signals are projected perpendicular to the ocean surface toward the ocean bottom. Acoustic energy is scattered back to the acoustic surface from particles or temperature and salinity fluctuations found in the vicinity of density discontinuities located at the boundary between layers of ocean water. Changes in the depth of the boundaries by fluid processes such as internal waves are extracted from changes in the roundtrip travel time of the scattered acoustic signals. As a result, the fluid process causing the changes can be visualized and studied.

Flow Visualization Images: A section of an internal wave packet detected by the acoustic flow visualization system (insert in Fig. 4) shows a downward displacement of the base of the ocean's mixed layer (scattering layer). The data were taken on the New Jersey Shelf.[1] The scattering layer was tracked for more than 27 km. The depth of the base of the mixed layer was digitized and is plotted (Fig. 4). Two features are present: the first is a vertical displacement of the mixed layer (arrow 1). It slowly recovers over a distance of 20 km. This is the internal tide that was propagating shoreward (arrow 2) at ~0.5 m/s. The internal tide is generated on each tidal cycle and is a repeatable ocean process. The short wavelength (100 to 300 m) displacements within the internal tide envelope are caused by internal wave packets. They are dominated by mode 1 internal waves. The repeated generation of the internal tide, when stratified waters are present, suggests that the temporal and spatial variability of the shelf sound speed field may be repeated on each tide.

As mentioned, the interfacial internal waves imaged in Fig. 4 were dominated by the mode 1 component of the internal wave field. This component causes the stratified layers and sound speed field to be vertically displaced in the same direction (upward or downward) together. In a multilayer fluid, interfacial mode 2 internal waves cause the upper and lower boundary of one of the fluid layers to be displaced in opposite directions. This causes the sound speed profile variability to be different than the mode 1-dominant case shown above. Figure 5 shows a mode 2 interfacial internal wave imaged on the New Jersey Shelf during the fall of 2000. The mode 2 internal waves shown are 150 to 200 m in length.

In addition to mode 1 and mode 2 internal wave perturbation of the sound speed field, the internal tide and associated internal waves can also contain shear instabilities that cause water between two dif-

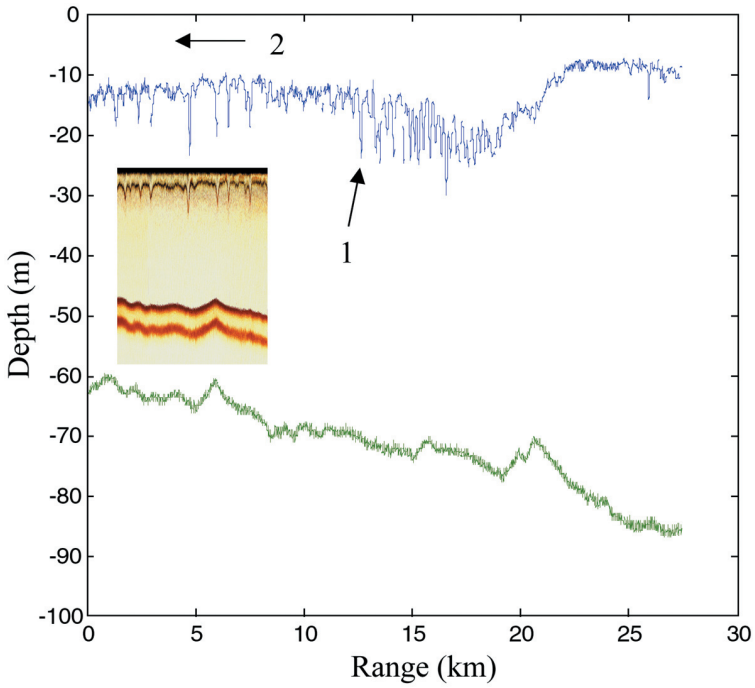

FIGURE 4
The range variability of the depth of an isosound speed layer (blue line) shows both long wavelength and short wavelength features. The ocean bottom is the green line. The direction of propagation of the internal tide, the 20-km depression feature, is shown by arrow 2. The insert shows a section of the acoustic flow visualization data that was digitized to obtain the 27-km realization of the sound speed variability. The vertical displacement of the mixed layer by the internal wave field is clear. The ocean bottom reflection is the upper red reflection. The lower bottom red reflection is an artifact. (From Fig. 24 of Ref. 1.)

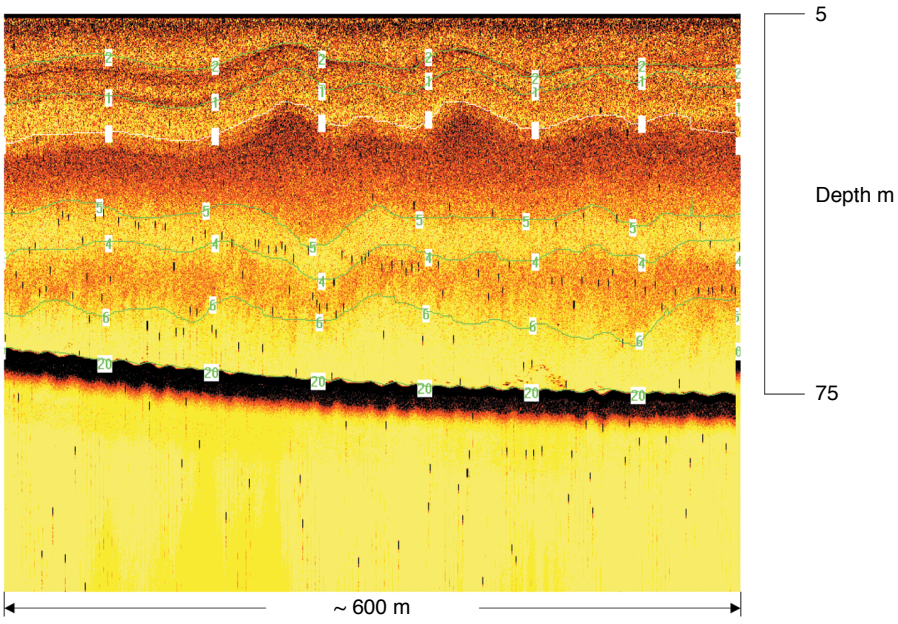

FIGURE 5
A 600-m flow visualization section showing the presence of a mode 2 internal wave on the New Jersey Shelf. The impact of mode 2 interfacial waves on the sound speed variability and acoustic signal variability is being addressed. Water depth is ~75 m.

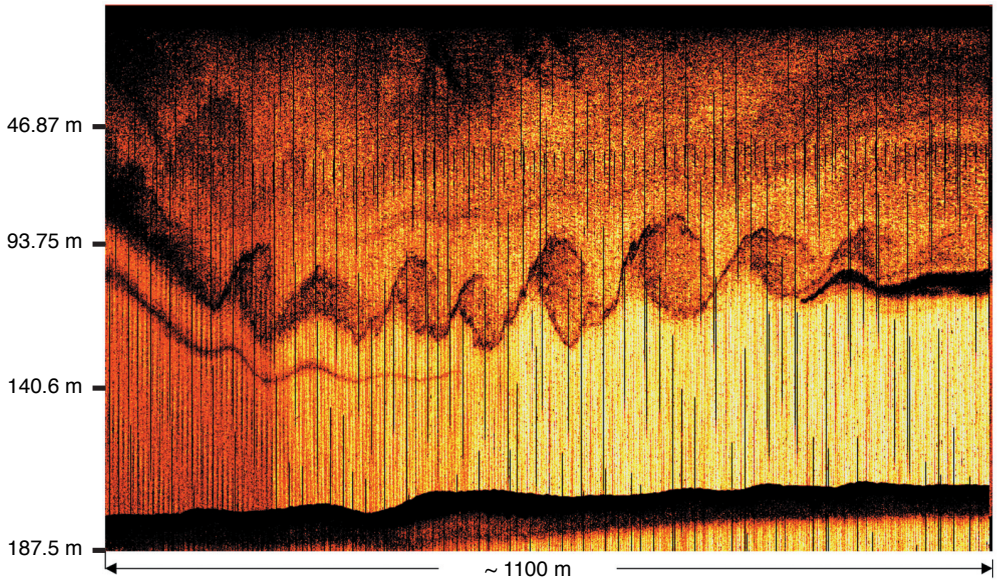

FIGURE 6
An 1100-m flow visualization record of a series of shear instabilities associated with the first lobe of a Luzon Basin soliton. Water between two layers is being mixed by roughly 40-m amplitude shear instabilities. This will cause short acoustic coherence lengths.

ferent fluid layers to mix. The mixing causes sound speed variability that will change the amplitude and phase of an acoustic signal that is propagating through the mixing event. Figure 6 shows a series of shear instabilities detected at the shelf break of the South China Sea. These instabilities were imbedded in the first lobe of an internal wave packet.

First-order calculations indicate that these instabilities could cause a perturbation to the complex properties of an acoustic signal propagating through them. The perturbation or variability is enough to cause an ~10 dB degradation in the performance of a large-aperture acoustic array.

Conclusions: High-frequency acoustic systems are being used to image the fluid processes generated by tidal flow over bathymetry. The fluid processes range in scale from 20-km internal tides to 10 m or less shear instabilities. The larger scale fluid processes appear to repeat on each tide. As a result, it may be possible to estimate the variability of the sound speed profile and naval array performance in littoral areas.

Acknowledgments: The low-noise preamplifier used in the acoustic flow visualization system was designed and integrated into the flow visualization system by Michael McCord. The following individuals helped with the development and installation of equipment and the acquisition of portions of the high-frequency data set: Earl Carey, Steve Wolf, Roger Meredith, James Schowalter, Bruce Pasewark, and John Kemp and his Woods Hole Oceanographic mooring group. We also thank the crews and staff of the UNOLS R/V *Endeavor* and the Taiwan research vessel *Ocean Research III* for their generous help.

[Sponsored by ONR]

Reference

[1] J.R. Apel, M. Baidey, C.-S. Chiu, S. Finette, R. Headrick, J. Kemp, A. Neuhall, M.H. Orr, B. Pasewark, D. Tielbuerger, A. Turgut, K. Von Der Heydt, and S. Wolf, "An Overview of the 1995 SWARM Shallow-Water Internal Wave Acoustic Scattering Experiment," *IEEE J. Oceanic Eng.* **22**, 465-500 (1997). ■

A Time-Domain Model for Acoustic Scattering from the Sea Surface

R.S. Keiffer
Acoustics Division

Introduction: It is common for sonar systems to operate under conditions in which (unavoidably) some of the sound generated by the source travels upward and impinges on the wavy ocean surface. If the seas are rough enough, a significant fraction of the energy hitting this boundary may scatter toward

the sonar receiver where it can act as a kind of noise that limits the sonar systems ability to detect a target. The current scientific literature contains descriptions of several computer models that can accurately predict the acoustic scattering from rough boundaries like the sea surface. These interface scattering models have overcome past difficulties presented by the broad band of spatial scales that exhibit significant roughness. However, a complete simulation of the surface reverberation problem must address the dynamic nature of the boundary and the inhomogeneity of the underlying medium. Difficulties in modeling these additional ocean-acoustic phenomena have kept the accurate calculation of the magnitude and spectral content of acoustic signals scattered from the sea surface as one of the outstanding unsolved problems in underwater acoustics.

Under the 6.1 Base Program, NRL has developed, benchmarked, and published the only computer model that predicts the 3-D acoustic scattering from sea surfaces in the time domain.[1] This model is called the Wedge Assemblage Scattering Program (WASP). Unlike some of the other highly accurate modeling approaches, it is efficient enough to be applied to the largest time-evolving 2-D sea surfaces of interest.

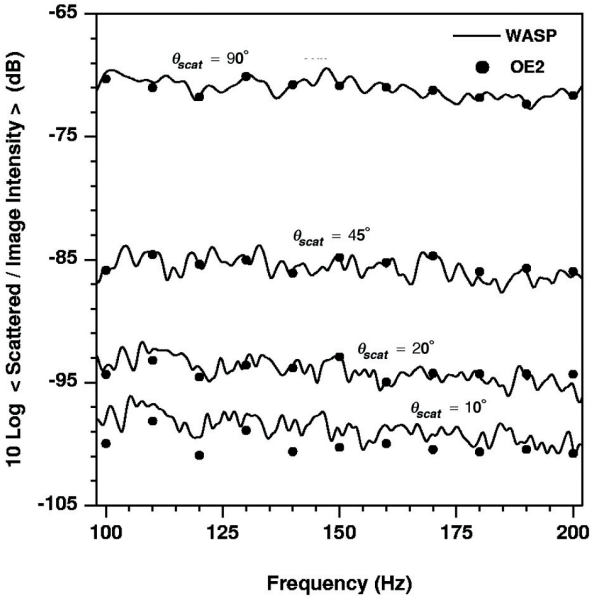

FIGURE 7
A comparison between the WASP model and a benchmark-accurate frequency domain solution (OE2) for the average intensity of sound backscattered from simulated 2-D seas that are due to a spatially uniform, steady, 20 m/s wind. The angle of insonification is 20° grazing and the scattered angles (θ_{scat}) are 90°, 45°, 20°, and 10° grazing.

Physical Basis of the Scattering Model: The basis of the WASP model is an exact time-domain solution for the scattered response of an impenetrable wedge-shaped boundary.[2] Because this solution has a clear and unambiguous physical interpretation, it is applicable (with some modification) to scattering problems involving complicated rough boundaries like the sea surface. NRL has extended this modeling approach from its original form for 1-D (corrugated) surfaces to fully 2-D surfaces. The WASP model for 2-D surfaces has been benchmarked against exact numerical solutions for scattering from simple objects (disks) and against highly accurate solutions for scattering from rough sea surfaces. Figure 7 shows results from this later benchmarking effort. Here we see comparisons between WASP and a benchmark-accurate frequency-domain solution for the average intensity of sound backscattered from simulated 2-D seas that are due to a 20 m/s wind. The angle of insonification is 20° grazing and the scattered angles (θ_{scat}) in the comparison are 90°, 45°, 20°, and 10° grazing. Of particular significance is the high level of agreement between WASP and the benchmark over the large dynamic range of scattered intensities.

Extension of WASP to Moving Surfaces: One of the promising attributes of the WASP model is the time-domain nature of its solution approach. While mathematically equivalent, frequency-domain solution approaches are, in practice, difficult to interpret under dynamic, time-varying conditions. The time-domain approach offers a conceptually straightforward algorithm for computing the scattered signal, even under circumstances in which the source, receiver, and surface all move in complicated ways. This motion induces an additional time variation in the scattered signal that manifests itself in the frequency domain as a frequency-shifting phenomenon called the Doppler effect. Using concepts from time-variant linear filter theory, the WASP model has been extended to address this dynamic scattering problem. Figure 8 shows an example of a simulation in which 2-D seas travel away from a static source and the backscattered signal is collected at a receiver that advances on the seas at a speed of 5 m/s. The WASP model supplies the average scattered power spectrum and the Doppler shift for a broad band of source frequencies. The modulation effect seen in this simulation is due to the receiver periodically (1 Hz) undergoing small excursions (1 m) up and down in the water as it advances on the seas.

Summary: NRL has developed and tested a unique time-domain scattering model that is being used to address many of the long-standing issues as-

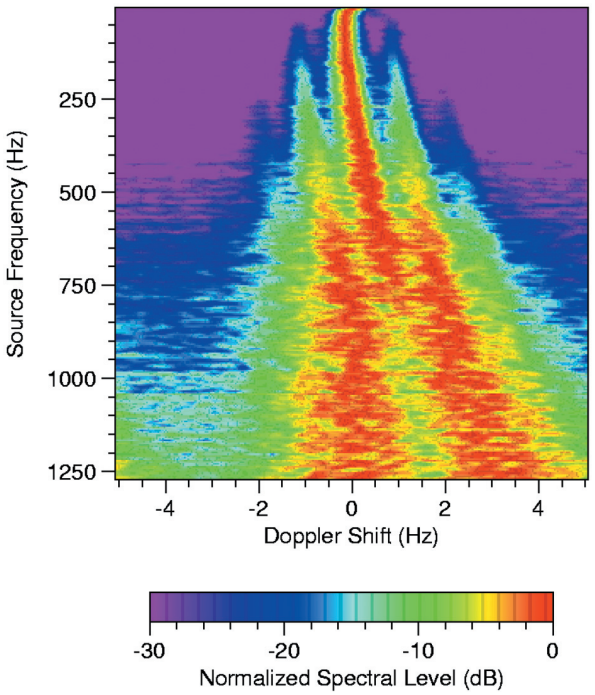

FIGURE 8
An example calculation made using the extension of the WASP model to moving surfaces. In this simulation, 2-D seas travel away from a stationary source and the backscattered signal is collected at a receiver that is advancing at a speed of 5 m/s while periodically (1 Hz) undergoing small (1 m) up and down excursions. The various motions involved cause frequency shifts in the average scattered power spectrum. This (Doppler) effect is calculated for a broad band of source frequencies. The modulation effect seen in this simulation is due to the periodic vertical displacement of the receiver.

sociated with acoustic scattering from dynamic ocean surfaces. Further development of this capability, along with more comprehensive acoustic and environmental data, will help mitigate the critical impact that sea surface reverberation can have on sonar performance.

Acknowledgments: The author acknowledges the many helpful conversations he has had with frequent co-author J.C. Novarini (Planning Systems Inc). Also, the author recognizes the grants of computer time at two DOD High Performance Computing Shared Resource Centers (Stennis Space Center, Mississippi, and Vicksburg, Mississippi).

[Sponsored by ONR]

References

[1] R.S. Keiffer and J.C. Novarini, "A Time-Domain Rough Surface Scattering Model Based on Wedge Diffraction: Application to Low-Frequency Backscattering from Two-Dimensional Sea Surfaces," *J. Acoust. Soc. Am.* **107**, 27-39 (2000).

[2] H. Medwin and C.S. Clay, *Fundamentals of Acoustical Oceanography* (Academic Press, New York, 1998), Chaps. 11-12.

Thin Profile, Low-Frequency, Underwater Electroacoustic Projectors

J.F. Tressler,[1] T.R. Howarth,[2] and W.L. Carney[3]
[1]*Acoustics Division*
[2]*Naval Sea Systems Command, Newport, RI*
[3]*Naval Sea Systems Command, Crane, IN*

Motivation: The Physical Acoustics Branch at the Naval Research Laboratory has been investigating a structural acoustic approach to detect and identify underwater mines.[1] This technique uses frequencies below 30 kHz to excite structural acoustic responses from the target. Through various algorithms, these structural clues can be converted into unique "fingerprints" that can be used to classify an unknown object as a mine. This low-frequency structural acoustic approach permits long-range detection as well as the ability to penetrate into sediment, which allows for the detection and identification of buried objects.

Because of their large size and weight, standard low-frequency source technologies are typically not adaptable for mounting on advanced underwater vehicles. An alternative technology, 1-3 piezoelectric ceramic-polymer composites, has the advantage of being thin and having low weight; however, its acoustic output at frequencies less than 10 kHz is lower than desired.

The Physical Acoustics Branch at the Naval Research Laboratory, in collaboration with the Naval Sea Systems Command, Divisions Crane and Newport, has designed and fabricated two projectors based on cymbal-type flextensional drivers. These projectors are thin enough for mounting on the side of an unmanned underwater vehicle and are capable of generating an adequate sound pressure level over the frequency band of interest.

Designs: *Cymbal Drivers*—Both projector designs use 294 miniature Class V flextensional electromechanical drivers laid out in a 14 × 21 square matrix. These drivers, known as "cymbals," consist of a piezoelectric ceramic disk that is mechanically and electrically coupled to two specially shaped titanium caps. The cymbals measure 12.7 mm in diameter and are approximately 2 mm thick (excluding the stud length). Figure 9 shows various views of these cymbal drivers.

Panel Projector—In the panel projector design, the cymbal drivers are sandwiched between two rigid graphite-epoxy composite cover plates. The cover plates have holes in them that allow the studs to pass through, thus allowing the cover plates to rest on the

FIGURE 9
The cymbal flextensional electromechanical driver.

apex of the cymbal caps. The plates are torqued onto the cymbals with nuts. The outer surface of each cover plate is electroplated with copper. The electrical connection is made to the piezoelectric ceramics via the electroplating, nuts, studs, and caps. A polyurethane gasket is stretched around the outside edge of the cover plates to maintain the interior air matrix after the projector is potted in polyurethane for waterproofing. The finished panel projector measures 350 × 248 × 15.9 mm and weighs 5 N in water.

Oil-filled Projector—In this design, the cymbal drivers are mounted within a molded sheet of 5-mm-thick neoprene rubber. Recessed cavities within the neoprene sheet hold each cymbal in place on its flat rim around the circumference of the disk. The 294 cymbals are connected electrically in parallel using thin nickel ribbon that is held on the studs by nuts. A single Plexiglas sheet, containing holes that align over the cymbals, is bonded to the upper and lower surfaces of the neoprene sheets. The Plexiglas provides a means to secure the cymbal-loaded neoprene sheet to the projector housing while assuring that the cymbal drivers remain in the same plane. Its dimensions are 381 × 280 × 64 mm and it weighs 26 N in water. This particular design has the added feature of resonance-frequency tunability, from between 6 and 10 kHz, which is done by adding or subtracting mass (i.e., nuts) from the cymbals.

Performance: Three projectors (two Panel and one Oil-filled) were mounted next to each other on one side of a fiberglass I-beam platform (Fig. 10) and evaluated in water. The three projectors were electrically connected together in series to improve impedance matching to the amplifier. Figure 11 shows the sound pressure level (SPL) achieved by the projector assembly from 700 Hz to 30 kHz when 300 V_{rms} (at one percent duty cycle) is applied to the system. An SPL over 180 dB (re: 1 µPa @ 1 m) is generated across the frequency band from 3 to 30 kHz. By applying an appropriate voltage at frequencies below 3 kHz, it would be possible to obtain a higher source level in this band. An SPL of 180 dB has been shown to continue up to at least 100 kHz as the ceramic radial resonance mode dominates at these upper frequencies.[2]

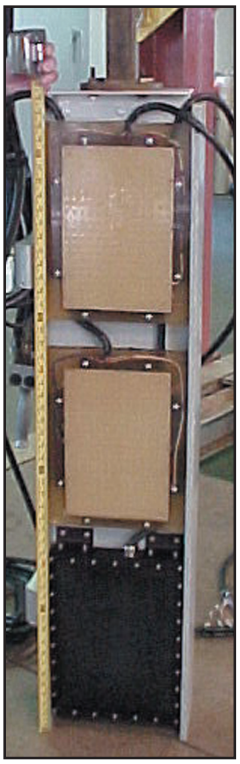

FIGURE 10
Cymbal panel projectors (top two) and oil-filled projector (bottom) mounted on a fiberglass I-beam.

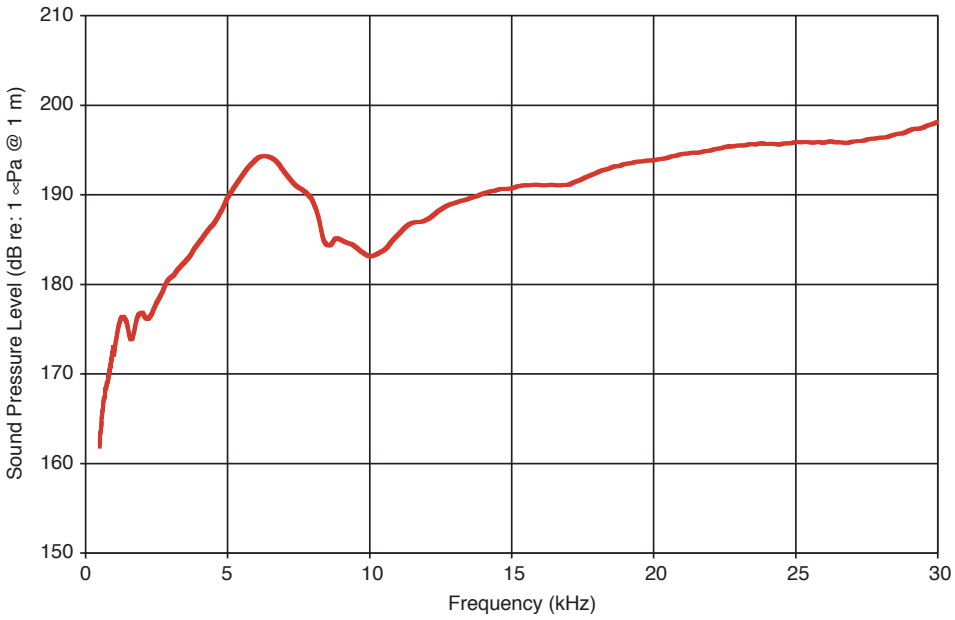

FIGURE 11
Sound pressure level generated by the projector assembly shown in Fig. 2 for a 300 V_{rms} drive level.

No competing source technologies are currently capable of producing such a high acoustic output over this entire frequency band within such a thin package. This marks a significant advance in low-frequency source technology, especially for use on future Navy vehicles.

Acknowledgments: The authors acknowledge the contributions of Bruce Johnson of ONR-321TS, Brian Houston of NRL, Joe Klunder of SFA, Inc., Kirk Robinson and Mel Jackaway of the Glendora Lake test facility, as well as Pat Arvin, Scott Small, and Phil Meadows of NSSC-Crane.

[Sponsored by ONR]

References

[1] T.J. Yoder, J.A. Bucaro, B.H. Houston, and H.J. Simpson, "Long Range Detection and Identification of Underwater Mines Using Very Low Frequencies (1-10 kHz)," in *Detection and Remediation for Mines and Minelike Targets III*, A.C. Dubey, J.F. Harvey, and J.T. Broach, eds. (SPIE, Bellingham, Washington, 1998), pp. 203-210.

[2] T.R. Howarth, J.F. Tressler, and W.L. Carney, "Oil-filled Cymbal Panels for Acoustic Projection Applications," *J. Acoust. Soc. Am.* **110**, 2753 (2001).